Neurocognitive and neuroanatomical maturation in the clinical high-risk states for psychosis: A pattern recognition study

Lana Kambeitz-Ilankovic[a,*,1], Shalaila S. Haas[a,b,1], Eva Meisenzahl[a,c], Dominic B. Dwyer[a], Johanna Weiske[a], Henning Peters[a], Hans-Jürgen Möller[a], Peter Falkai[a], Nikolaos Koutsouleris[a]

[a] Department of Psychiatry and Psychotherapy, Ludwig-Maximilian-University, Munich, Germany
[b] International Max Planck Research School for Translational Psychiatry (IMPRS-TP), Munich, Germany
[c] LVR-Klinikum Düsseldorf, Kliniken der Heinrich-Heine-Universität Düsseldorf, Germany

A B S T R A C T

Background: Findings from neurodevelopmental studies indicate that adolescents with psychosis spectrum disorders have delayed neurocognitive performance relative to the maturational state of their healthy peers. Using machine learning, we generated a model of neurocognitive age in healthy adults and investigated whether individuals in clinical high risk (CHR) for psychosis showed systematic neurocognitive age deviations that were accompanied by specific structural brain alterations.

Methods: First, a Support Vector Regression-based age prediction model was trained and cross-validated on the neurocognitive data of 36 healthy controls (HC). This produced Cognitive Age Gap Estimates (CogAGE) that measured each participant's deviation from the normal cognitive maturation as the difference between estimated neurocognitive and chronological age. Second, we employed voxel-based morphometry to explore the neuroanatomical gray and white matter correlates of CogAGE in HC, in CHR individuals with early (CHR-E) and late (CHR-L) high risk states.

Results: The age prediction model estimated age in HC subjects with a mean absolute error of ± 2.2 years (SD = 3.3; $R^2 = 0.33$, $P < .001$). Mean (SD) CogAGE measured + 4.3 (8.1) years in CHR individuals compared to HC (-0.1 (5.5) years, $P = .006$). CHR-L individuals differed significantly from HC subjects while this was not the case for the CHR-E group. CogAGE was associated with a distributed bilateral pattern of increased GM volume in the temporal and frontal areas and diffuse pattern of WM reductions.

Conclusion: Although the generalizability of our findings might be limited due to the relatively small number of participants, CHR individuals exhibit a disturbed neurocognitive development as compared to healthy peers, which may be independent of conversion to psychosis and paralleled by an altered structural maturation process.

1. Introduction

Neurocognitive deficits are a hallmark of first-episode psychosis and they are predictive of poor functional outcome many years later (Albus et al., 2006). Executive, attentional and mnemonic impairments have been traditionally attributed to established psychotic illness, but studies have compiled compelling evidence for neurocognitive abnormalities paralleling the emergence of cognitive-perceptual basic symptoms in a putative 'early' clinical high-risk state (CHR-E) and the appearance of attenuated psychotic symptoms in a 'late' ultra-high risk (CHR-L) state for psychosis (Keefe et al., 2006; Pukrop et al., 2006; Ziermans et al., 2014). In addition, recent work has suggested that these abnormalities follow a gradient from typically developing children and adolescents to peers showing psychosis-spectrum symptoms (Gur et al., 2014). Both sets of findings emphasize the role of neurocognitive abnormalities as a proxy for altered neurodevelopmental trajectories underlying the emergence of psychosis (Pantelis et al., 2005; Rapoport et al., 2012).

Previous neuroimaging studies have suggested that these complex brain-behavioral trajectories may best be modeled by means of multivariate pattern analysis (MVPA) (Koutsouleris et al., 2012a). Machine learning techniques have successfully been applied to structural MRI scans to predict age of healthy volunteers (Su et al., 2012). This research has been essential in understanding and creating normative trajectories of brain development (Erus et al., 2015). Moreover, MVPA has been employed in studies showing acceleration of normal brain maturational processes (Koutsouleris et al., 2014; Schnack et al., 2016) that appears to be an intermediate phenotype for psychosis (Gogtay, 2008) and disrupts the normal process of gray (GM) and white matter (WM) maturation, potentially continuing to alter brain-behavior trajectories during early adulthood (Cropley et al., 2016).

The cognitive lag in adolescents at risk for psychosis observed relative to their chronological age is commonly due to slower cognitive

---

development in the cognitive domains of verbal reasoning and social cognition (Green et al., 2015; Gur et al., 2014; Lin et al., 2011) and decline in these cognitive domains usually overlap with those reported in adult CHR individuals (Lin et al., 2011) and patients with established psychotic disorders (Green et al., 2015). Nonetheless, cognitive lag in adolescents at risk for psychosis seems not to be equally and continually represented in all cognitive domains and age ranges, pointing to a rather dynamic interplay between structural brain maturation and cognitive development across this life period.

To date, it is still unclear whether the delay of neurocognitive maturation observed in CHR adolescents (Gur et al., 2014) continues into adulthood. We used supervised machine learning to train and cross-validate an individualized age predictor in healthy volunteers using their multivariable neurocognitive data. The model was then applied to the respective neurocognitive data of our CHR patients to investigate systematic differences between neurocognition (NC)-based predicted age and calendar age (Cognitive Age Gap Estimation; CogAGE) as compared to the healthy reference population. While our NC model ought to explain the relationship between age and predicted age, we were further interested in characterizing how CogAGE alters with respect to calendar age of CHR individuals. We assumed that CogAGE, as the measure of delay in neurocognitive development, is going to significantly differ between CHR-L and CHR-E individuals.

We aimed to investigate whether neurocognitive maturation was altered in CHR individuals and accompanied by specific brain alternations as compared to a healthy adult population. As previous findings suggest that GM volume is an important intermediate phenotype for the assessment of brain development and cognition (Gennatas et al., 2017), this highlights the need for combined studies that further investigate their associations. In addition, we tested if the use of entire NC battery was justified for multivariate CogAGE modeling.

2. Methods

2.1. Participants

Forty-eight individuals with a clinical high-risk state and 36 age- and sex-matched healthy controls were recruited at our Early Detection and Intervention Centre for Mental Crises (FETZ) of the Department of Psychiatry and Psychotherapy, Ludwig-Maximilian-University, Germany. Potential CHR individuals were referred to our center by primary, secondary and tertiary mental healthcare services and were examined according to a standardized inclusion and exclusion criteria checklist with operationalized definitions as described previously (Koutsouleris et al., 2012; Meisenzahl et al., 2008). All participants underwent neuropsychological testing using a comprehensive battery (Table 1). Except for five CHR patients, this sample was also examined using structural MRI scanning.

In summary, study inclusion required either CHR-E with a positive global functioning and trait marker defined by a ≥ 30 point reduction in the DSM-IV Global Assessment of Functioning Scale (GAF), and a family history of psychotic disorders or a personal history of pre-/perinatal complications, or at least 1 positive psychopathological state marker in the basic symptoms (Klosterkötter et al., 2001), or (Keefe et al., 2006) CHR-L exhibiting attenuated psychotic symptoms (APS) or brief limited intermittent psychotic symptoms (BLIPS) categories fulfilling specific duration criteria (Yung et al., 1998). Of the forty-eight CHR patients, 19 fulfilled basic symptom criteria and were therefore assigned to a putative 'early' Clinical High-Risk state (CHR-E), whereas the other 29 individuals showed attenuated (APS) and/or brief limited intermittent psychotic (BLIPS) symptoms as operationalized by the UHR criteria of the Personal Assessment and Crisis Evaluation (PACE) clinic in Melbourne (Yung et al., 2003; Yung et al., 2004), and therefore were labeled as 'late' Clinical High-Risk State (CHR-L) individuals. Exclusion criteria were assessed for the candidate CHR and HC individuals by evaluating the personal and familial history using a semi-structured

clinical interview as well as the Structured Clinical Interview for DSM-IV (American Psychiatric Association, 2000). Additionally, patients were rated using the Positive and Negative Symptom Scale (PANSS) (Kay et al., 1987) and the Montgomery-Åsberg Depression Rating Scale (MADRS) (Montgomery and Asberg, 1979) (Table 1.) All participants were followed-up for 4 years after this assessment for transition to psychosis. They provided written informed consent prior to study inclusion and the study was approved by the Local Research Ethics Committee of the Ludwig-Maximilian-University.

2.2. Neurocognitive testing

A cross-domain neuropsychological test battery comprising 9 standardized tests was administered to all subjects (Table 1). The neurocognitive battery includes tests measuring domains of premorbid IQ, processing speed, attention verbal and spatial working memory, verbal memory and mental flexibility yielding measures of accuracy (number of correct responses) and speed (time of execution). We used a strong apriori approach when designing the battery relaying on previous studies of large scientific consortia investigating neuropsychological functioning in schizophrenia — Matrics Cognitive Concensus Battery (Marder and Fenton, 2004) and Philadelphia Neurodevelopmental Cohort (PNC) (Moore et al., 2015).

Fourteen test variables were computed across the HC group (Table 1) and adjusted for the effects of age and gender using partial correlations. The adjusted scores were z-transformed based on the respective HC data and entered analyses of variance (ANOVAs) that assessed between-group differences in HC vs CHR individuals. Holm's sequential method (Holm, 1979) was used to adjust P values for multiple comparisons across the 14 neurocognitive measures and significance was defined at $P < .05$, corrected.

All subjects had never received neuroleptic agents prior to MRI and clinical examination. The neuropsychological test battery used to examine neurocognitive functions in these subjects has previously been described in detail (Koutsouleris et al., 2010).

2.3. Support vector regression for neurocognitive-based age prediction

Support vector regression (SVR) (Montgomery and Asberg, 1979) was chosen due to its established ability to generate unbiased models that generalize well across the population, as shown in our previous study investigating accelerated brain ageing (Koutsouleris et al., 2014). To train and cross-validate our models, we wrapped our machine learning pipeline into a nested CV framework as described in our previous work (Cabral et al., 2016; Koutsouleris et al., 2015) using our open-source machine learning tool NeuroMiner (https://www.pronia.eu/neurominer/). More specifically, for the present study we defined a leave-one-subject-out cross-validation cycle at the outer cross-validation cycle (CV_2) and a repeated 10-by-10-fold cross-validation at the inner cycle (CV_1). This maximized the data available to the machine learning process while both generating robust parameter estimates and avoiding any overfitting of the machine learning pipeline to our HC data. Each training sample at the CV_1 loop was first processed using feature-wise standardization. Then, the standardized neurocognitive data were projected into a linear kernel space, where the SVR algorithm determined an optimal age-fitting function at a fixed C (regularization) parameter of 1 and a ν-parameter, which was optimized in the range of [0.5 0.7 0.9] within the CV_1 cycle. To this end, NeuroMiner generated CV_1 test partition predictions across the ν range and then picked the optimal ν at the parameter showing the lowest average Mean Absolute Error (MAE) across the respective CV_1 cycle. The 10×10 CV_1 models trained with this ν parameter were then applied to the respective CV_2 subject and the resulting age predictions were averaged to obtain a final out-of-training-sample prediction for a given participant. Finally, to correct for the over- and underestimation of age in the lower and upper tails of the distribution as typically encountered in SVR, we computed

Table 1
Demographics, clinical characteristics and neurocognitive test performance.

	HC	CHR-E	CHR-L	F/X^2	P
Sociodemographic variables:					
N	36	19	29	–	–
Age: mean (SD) [years]	27.16 (3.71)	25.2 (5.68)	24.35 (5.88)	0.90	0.41
Gender: male/female (%)	19/17 (52.77/47.22)	12/7 (63.16/36.84)	20/9 (68.97/31.03)	1.66	0.20
School education: mean (SD) [years]	12.53 (1.13)	12.22 (1.06)	11.75 (1.24)	3.58	0.03
Clinical variables: mean (SD)					
GAF score	–	61.75 (8.77)	54.21 (12.95)	2.91	0.10
PANSS total score	–	58.08 (14.68)	68.36 (25.71)	1.49	0.23
PANSS positive score	–	10.00 (2.66)	14.21 (5.07)	6.68	0.02*
PANSS negative score	–	15.58 (7.10)	19.14 (9.59)	1.12	0.30
PANSS general score	–	32.50 (8.42)	35.00 (12.78)	0.33	0.57
MADRS	–	18.58 (8.28)	17.43 (10.81)	0.91	0.77
Neuropsychological variables: standardized Z scores					
Premorbid IQ	0.23 (0.41)	0.09 (0.67)	−0.02 (0.68)	1.48	0.23
Mehrfach-Wortschatztest B (MWT-B) - Raw score					
Digit Symbol Substitution Test (DSST, WAIS-III) - Raw score correct	−0.05 (0.96)	−0.18 (1.03)	−1.15 (1.17)	9.62	0.00*
Digit Span Test (DS, WAIS-III) - Raw score correct	−0.03 (0.93)	0.08 (1.14)	−0.29 (1.17)	0.81	0.45
Letter Number Span Test (LNS) - Raw score correct	0.08 (0.96)	−0.13 (2.37)	−1.30 (2.96)	3.51	0.04*
Trail-Making Test, part A (TMT-A) - Time to completion (s)	0.06 (0.97)	−0.14 (1.25)	−1.02 (1.50)	6.50	0.02*
Trail-Making Test, part B (TMT-B) - Time to completion (s)	−0.03 (0.95)	−0.93 (1.51)	−2.05 (1.95)	14.87	0.00*
Difference between TMT-B & TMT-A (TMT-B-A)	−0.06 (0.97)	−0.96 (1.42)	−1.78 (1.87)	11.59	0.00*
Trail-Making Test, TMT (part B/part A; BdivA)	1.66 (5.21)	−2.02 (12.53)	−2.02 (12.53)	1.66	*0.03
Trail-Making Test, TMT (part B − part A/part A; B-AdivA)	0.66 (5.21)	−3.02 (12.53)	−3.02 (12.53)	1.66	*0.03
Self-Ordered Pointing Task (SOPT) - Error score	−0.04 (0.98)	−2.58 (3.03)	−2.28 (2.11)	14.49	*0.00
Rey Auditory Verbal Learning Test (RAVLT)					
Sum of raw score correct after trials 1–5 (RAVLT-IR)	0.15 (0.96)	−0.75 (1.21)	−1.96 (2.12)	15.71	*0.00
Raw score corrects after delayed recall (RAVLT-DR)	0.08 (0.92)	−0.79 (1.54)	−2.38 (2.99)	12.39	*0.00
Retention: difference between raw score correct in trial 5 and delayed recall (RAVLT-Ret)	0.03 (0.94)	−0.81 (1.45)	−0.90 (2.19)	3.27	*0.04
Verbal Fluency - Sum of correct responses (letters) (VF)	−0.02 (0.85)	−0.03 (1.42)	−0.55 (1.50)	1.73	0.18

Significance was defined as $p < .05$.
* Tests that survive Holm's sequential method to correct for multiple comparisons.

detrending parameters by fitting the CV_2 subjects' age residuals with their chronological age.

The scaled and imputed training matrix entered a greedy forward search wrapper (early stopping at 50% of features) (Saeys et al., 2007), to identify the most parsimonious subset of variables within the pool of neuropsychological tests.

The out-of-training prediction performance was quantified using the MAE and explained variance (R^2). To obtain age predictions for the CHR group we applied all pre-computed standardization, SVR and detrending models to the CHR individuals' neurocognitive data. Finally, we calculated all participants' CogAGE scores as the difference between estimated neurocognitive and observed chronological age. In addition, to evaluate the predictive potential of solely premorbid IQ we used the General Linear Model (GLM) and the same cross-validation scheme as in the neuropsychological model with all 14 measures.

2.4. MRI data acquisition and preprocessing

Magnetic resonance images were obtained on a 1.5 T Magnetom Vision scanner (Siemens, Erlangen, Germany) using a T1-weighted 3D-MPRAGE sequence (repetition time (TR) 11.6 ms, echo time (TE) 4.9 ms, field of view 230 mm, matrix 512 × 512, 126 contiguous axial slices of 1.5 mm thickness, voxel size 0.45 × 0.45 × 1.5 mm). All images were examined for image artifacts, gross anatomical abnormalities, and signs of neurological disease by trained clinical neuroradiologists.

Structural MRI data were preprocessed using the CAT12 toolbox (http://www.neuro.uni-jena.de/cat/), an extension of the SPM12 software (Wellcome Department of Cognitive Neurology, London, UK; http://www.fil.ion.ucl.ac.uk/spm/software/spm12/). The CAT12 toolbox extends the unified segmentation model into GM, WM and cerebrospinal fluid (CSF), executed through SPM12 (Ashburner and Friston, 2005) from Welcome Department of Clinical Neurology running on MATLAB2015a (The MathWorks, Natick, MA, USA) by 1)

applying an Adaptive Maximum a Posterior (AMAP) technique, based on modeling local parameter variances as spatial functions (Rajapakse et al., 1997), 2) performing a Partial Volume Estimation (PVE), which estimates the ratio of pure tissue types in each voxel (Tohka et al., 2004) and 3) denoising using a classical Markov Random Field model (Rajapakse et al., 1997) for post-processing. A second denoising method employed after intensity normalization is a Spatial-Adaptive Non-Local Means (SANLM) filter (Manjón et al., 2010). The DARTEL algorithm (Ashburner, 2007) was used to normalize the GM and WM maps to the MNI (Montreal Neurological Institute) structural template. Final images were modulated with the Jacobian determinant generated through non-linear spatial normalization and lastly smoothed with a 4-mm Full-Width-at-Half-Maximum Gaussian kernel.

2.5. Statistical analysis

Sociodemographic and clinical characteristics were tested for between-group differences (HC, CHR-E, CHR-L) using independent sample *t*-tests for continuous data, ANOVA and Fisher's exact test for categorical data in SPSS (IBM Corp. Released 2013. IBM SPSS Statistics for Windows, Version 22.0. Armonk, NY: IBM Corp.). The regression slopes indicating differences in calendar age and predicted age between HC and CHR (CHR-E and CHR-L) were calculated in SPSS by deriving SVR decisions scores from Neurominer. Subsequently, to test for the differences in the regression slopes when comparing performance of the NC model versus the model with solely premorbid IQ, Cocor R (Diedenhofen and Musch, 2015) package was used.

2.5.1. Correlational analysis CogAGE scores with GM and WM volume

A multiple regression model across all participants was set up to identify brain regions in which voxel-level, whole-brain GM and WM volume alterations were related to CogAGE scores. In addition, we included total intracranial volume (TIV) as regressor into the multiple regression design to correct for global brain volume variation
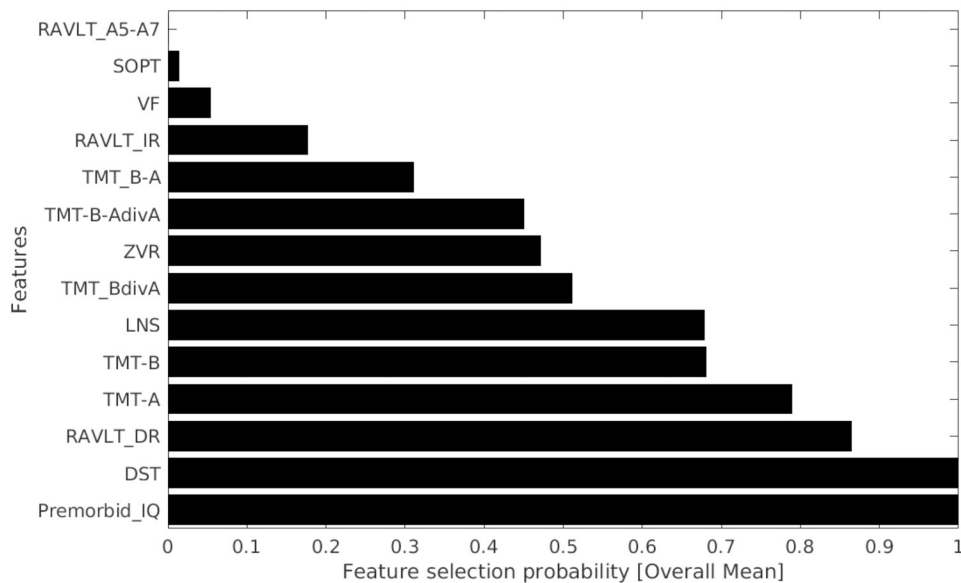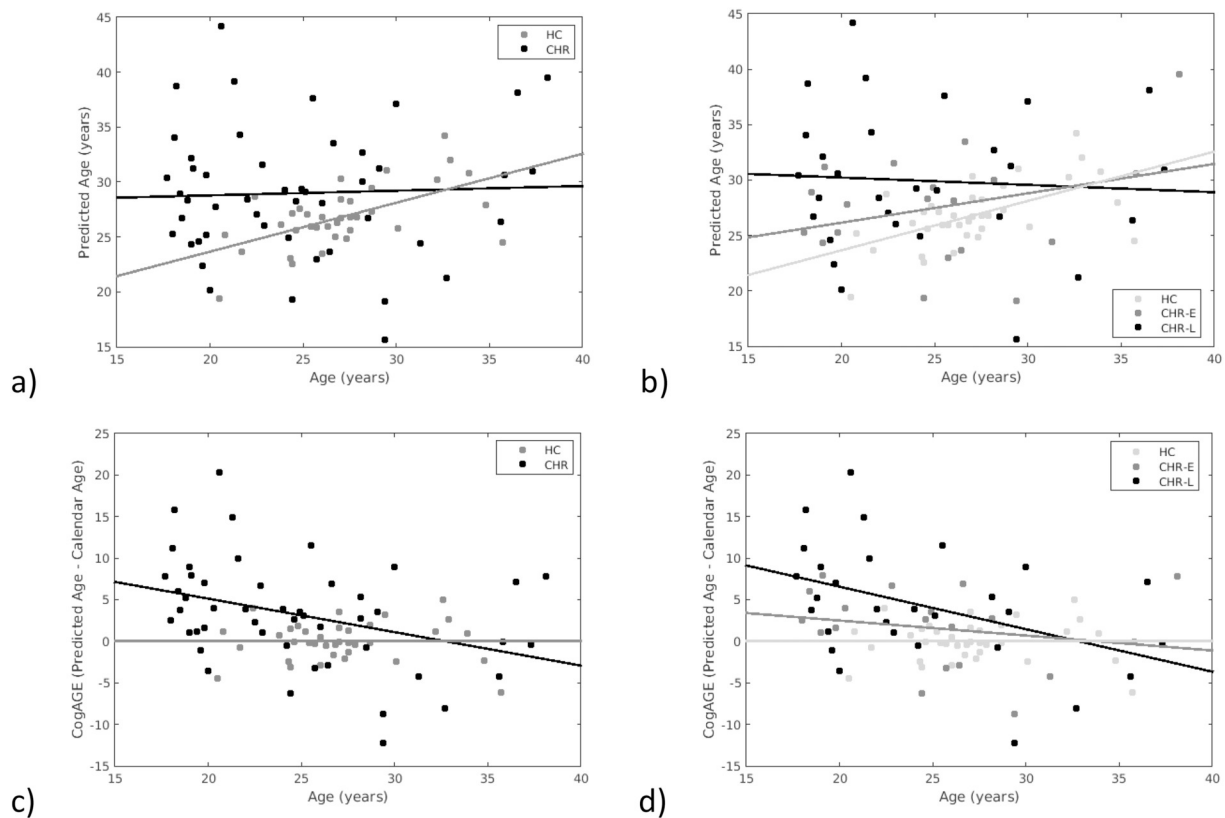
Fig. 1. The relationship between age and predicted age a) in HC and CHR group b) HC, CHR-E, and CHR-L. The model illustrating the relationship between age and cognitive Age Gap Estimator (CogAGE) c) in HC and CHR group d) HC, CHR-E, and CHR-L; and e) the selection probability of neuropsychological measures derived from SVM model generated for predicted age.

RAVLT_A5-A7, Rey Auditory Verbal Learning Test – Retention; SOPT, Subject-Ordered Pointing Task; VF, Verbal Fluency; RAVLT_IR, Rey Auditory Verbal Learning Test – Immediate Recall; TMT_B-A, Trail-Making Test Part B minus Part A; TMT-B-AdivA, Trail-Making Test Part B minus Part A divided by A; TMT-BdivA, Trail-Making Test Part B divided by A; ZVR,Digit Span Forwards and Backwards; LNS, Letter Number Span; TMT-B, Trail-Making Test Part B; TMT-A, Trail-Making Test Part A; RAVLT-DR, Rey Auditory Verbal Learning Test – Delayed Recall; DST, Digit Symbol Test.

introduced by modulating the GM tissue maps during pre-processing.

The positive contrast indicated relationship between GM and CogAGE whereas the negative contrast indicated relationship between WM and CogAGE scores. To sensitize our neuroanatomical analysis both for large focal and subtle, spatially contiguous effects, we used Threshold-Free Cluster Enhancement (TFCE) (Smith and Nichols, 2009) as implemented in the SPM TFCE toolbox (http://dbm.neuro.uni-jena.de/tfce/). We performed $N = 2000$ permutations of each previously generated contrast. Statistical significant effects in the TFCE maps were defined at $P < .05$ corrected for multiple comparisons using the

family-wise error rate (FWE).

3. Results

The age prediction model estimated age in HC subjects with a mean absolute error of 2.2 years (SD = 3.3; r^2 = 0.33, P < .001). Mean (SD) CogAGE measured +4.3 (8.1) years in CHR individuals compared to HC (−0.1 (5.5) years, P = .006) (Fig. 1a and b). The ANOVA model showed that CHR-L differed significantly from HC, (+5.6(9.0) years; P = .003) while this was not the case for the early CHR-E group (+2.3 (6.3) years; P = .234). Compared to HC, CogAGE was increased both in converters (+5.5 (4.5) yrs.; P = .005) and non-converters (+4.0 (6.6) yrs.; P < .001) to psychosis. The multiple regression model confirmed (Fig. 1c) a negative relationship between CogAGE and age in CHR group (R^2 = −0.36, P = .01) as compared to HC volunteers that seems particularly driven by CHR-L (R^2 = −0.43, P = .02) and not CHR-E (R^2 = −0.21, P = .38) group (Fig. 1d). Additionally, the negative relationship between CogAGE and chronological age in CHR patients appears to be undoubtedly more pronounced in younger CHR patients. The highest selection probability in CogAGE modeling was achieved for the neuropsychological test measuring Premorbid IQ and Digit Symbol Substitution (DSST) Test (Fig. 1e).

Therefore, we also investigated predictive potential of solely Premorbid IQ and DSST as the most relevant features among the 14 neuropsychological measures in the study. Predicting chronological age based on IQ scores yielded significant results in the group of HC volunteers (r = 0.472, p = .003) similarly to model using all the 14 features, yet the IQ model was equally generalizable to CHR group (r = 0.270, p = .064) and therefore unable to detect CogAGE discrepancy in CHR group. This contrasts to our initial findings using all NC model with 14 neurocognitive tests, which was able to show a significant difference between the slopes of the HC and CHR models (z = 2.6853, p-value = .0072). The model based on DSST failed to predict age in healthy volunteers (r = 0.13, p = .43) when used segregated from the rest of the neuropsychological battery and therefore was not further applied to CHR patients.

The multiple regression models performed on CogAGE scores of all HC and CHR individuals and neuroanatomical data revealed significant clusters of volume increase and decrease in multiple brain areas (Fig. 2a). Across the sample CogAGE was positively correlated with the increased GM volume in left cingulate gyrus, left superior temporal gyrus followed by left superior and middle frontal gyrus, whereas positive correlations on the right hemisphere were identified in the angular and supramarginal gyrus. Further positive correlations were found in the superior temporal gyrus and frontopolar cortices, in the right hemisphere. Whilst higher CogAGE scores across the sample were associated with increased GM volume, they were also correlated with a significant WM volume decrease within the middle cerebellar peduncle of the right hemisphere left genu and the splenium of the corpus callosum (CC), as well as the third branch of the right superior longitudinal fasciculus (SLF III) of the right hemisphere (Table 2). The associations between the CogAGE and cingulum as the first GM eigenvariate and respectively between middle cerebellar peduncle as the WM eigenvariate from the multiple regression model are shown in scatterplots of the Fig. 2b and c. The correlations between remaining GM and WM eigenvariates can be found in the supplementary materials.

4. Discussion

In this study, we investigated whether neurocognitive maturation was altered in CHR individuals and accompanied by specific brain changes as compared to a healthy control population. Although a majority of studies showed that both cognitive impairment and brain alterations are commonly found in CHR individuals, only one study so far has investigated how neurocognitive trajectories evolve during adolescence (Gur et al., 2014), but not in the early adulthood of CHR individuals. In line with the results of this neurodevelopmental population study that demonstrated neurocognitive delay in adolescents with psychosis-spectrum symptoms, we were able to show discrepancy between calendar age and neurocognitive age, suggesting delayed neurocognitive development in young CHR adults.

Whilst our results suggest that CogAGE is more pronounced in the younger individuals from the CHR sample, the CogAGE delay seems to stabilize if the patients fulfilling CHR criteria are in their early thirties. This observation may suggest that CogAGE captures neurocognitive delay, rather than a static cognitive impairment that is usually associated with early psychosis spectrum disorders. Additionally, the negative relationship between CogAGE and chronological age in CHR patients appears to be undoubtedly more pronounced in CHR-L patients than in CHR-E patients. Notably, the subgroup analysis of CHR patients with vs. without transition to psychosis did not yield any significant results in this regard.

Our finding that CHR patients' premorbid IQ and processing speed measures were most relevant for the age prediction provides further hints to a potential dysmaturational process in these individuals. Namely, a cross-sectional study of cognitive maturation in healthy subjects indicate maturation of processing speed through late childhood and into adolescence (Luna et al., 2004). The improved speed of performance could be attributed to increased efficiency in neuronal organization and communication through myelination and pruning processes. Previous studies on adolescent-onset psychosis patients failed to show normal age-related increases in processing speed, which is in keeping with the findings in our CHR patients (Erus et al., 2015; Bachman et al., 2012). The premorbid IQ has always been strongly associated with risk for psychosis and used as one of the main arguments for a widespread neurodevelopmental hypothesis of the disorder (Khandaker et al., 2011; Reichenberg et al., 2002). Though the premorbid measure of intelligence and digit symbol substitution test proved to be strongly relevant for the age prediction, they were insufficient when used separately from other neuropsychological measures. The SVR model including all the neuropsychological measures was able to detect subtle relationships between the features that would not be detectable at a univariate level.

The neural changes subserving the growing complexity of cognitive functions in response to higher environmental demand (Pantelis et al., 2005; Gogtay, 2008) occur in a non-linear fashion which seems to be supported by our findings. At the neuroanatomical level, CogAGE seems to be associated with a distributed pattern of increased GM volume particularly in the temporal and frontal areas of both hemispheres. The sequence of cortical GM loss that normally occurs earliest in the primary sensorimotor areas and latest in the dorsolateral prefrontal cortex is disrupted in psychosis along with the intra-cortical myelination processes (Peters and Sethares, 2004). Most studies suggest that the brain changes in psychosis may represent a dysregulation of the temporal course of neurodevelopmental trajectory (Lieberman, 1999; Woods, 1998). Our results on delayed GM loss in frontal brain regions support the notion about the active disease process occurring early in the course of illness and changing the temporal course of neural development. Additionally, it could be interpreted as a compensatory neural process taking place in the brains of CHR patients as a result of cortical reorganization.

The positive associations between CogAGE and GM and their interactions with psychosis proximity and chronological age may point to a delay of the neuroanatomical maturation sequence described above conditional on the time of symptom onset between adolescence and adulthood. This interpretation is supported by our finding on WM reductions in the right middle cerebellar peduncle. This result on volume decrease in the cerebellar WM pathways supports our hypothesis of delayed brain structural and neurocognitive development in CHR patients as compared to cerebellar maturation in healthy peers (Tiemeier et al., 2010; Sussman et al., 2016). Importantly, in contrast to an
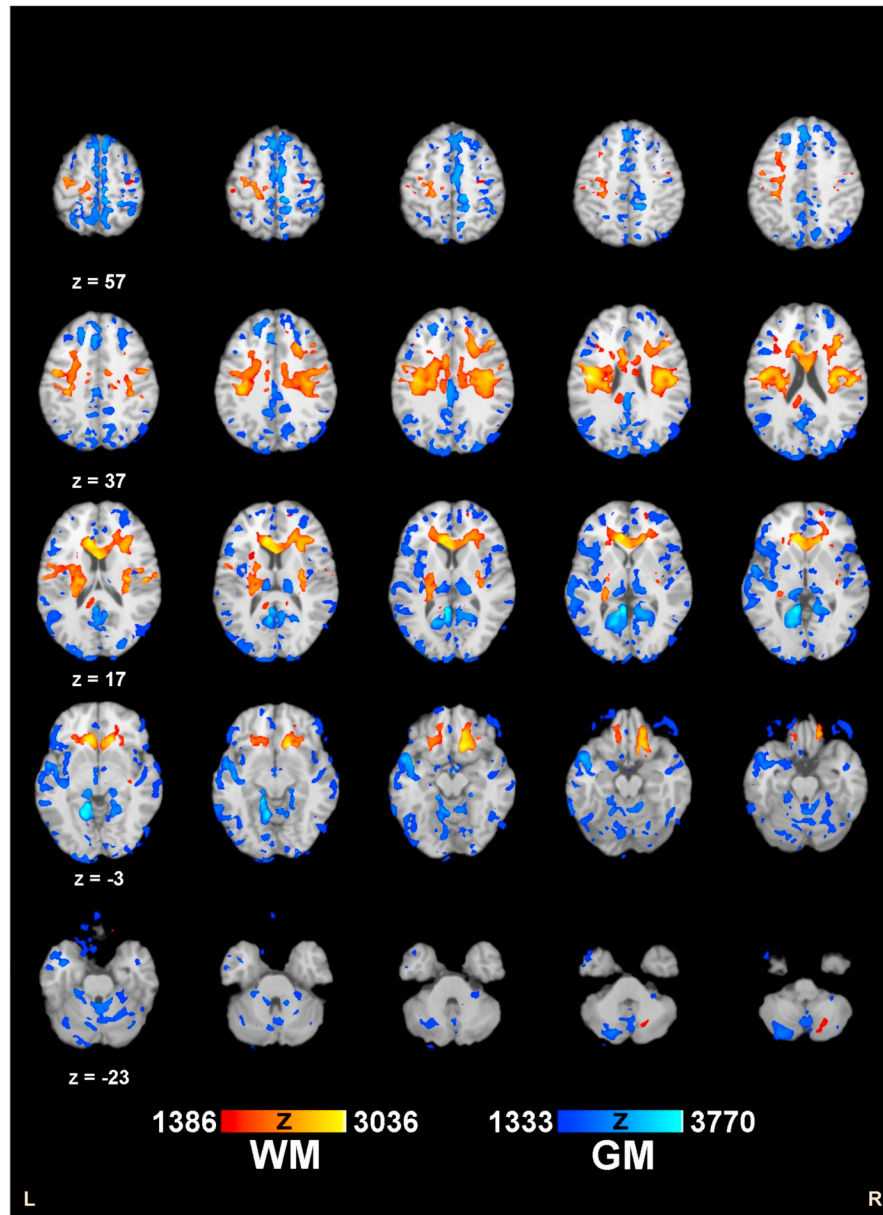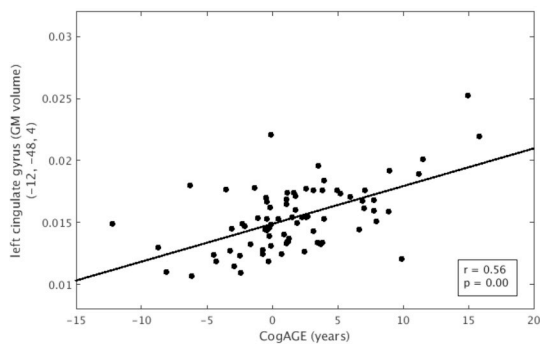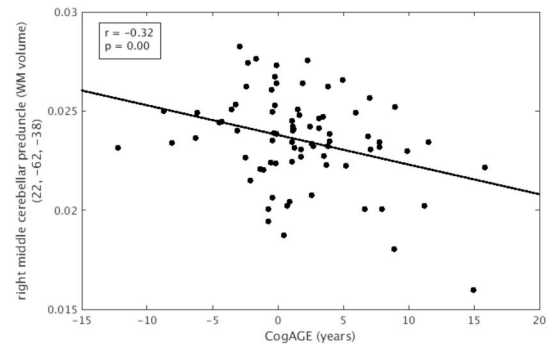
Fig. 2. The multiple regression models showing relationship between CogAGE scores and neuroanatomical data across the sample in a) increased GM volume regions (blue) that are positively correlated with CogAGE scores and decreased WM volume (red) regions that are negatively correlated with CogAGE; b) the first eigenvariate (left cingulate gyrus) extracted from the multiple regression model in GM (adjusted CogAGE scores); c) in the second eigenvariate extracted (right middle cerebellar peduncule) from the multiple regression model in WM (adjusted CogAGE scores).

Table 2

Brain regions significantly correlated with CogAGE scores in GM (positive correlation) and WM (negative correlation) volume across CHR and HC individuals.

	Brain region	Left/Right	Cluster Size (voxels)	MNI Coordinates of local maxima (mm)			P-value
				x	y	z	
Gray Matter	Cingulate gyrus	L	206,461	−12	−48	4	0.001
	Superior temporal gyrus	R	7655	46	−18	−2	0.009
	Middle frontal gyrus	L	588	−30	52	8	0.014
	Superior temporal gyrus	L	1419	62	−20	0	0.020
	Cerebellum Crus II	R	167	36	−68	−42	0.020
	Superior frontal gyrus	L	366	−18	56	8	0.025
	Frontal pole	L	273	−2	54	−24	0.031
	Rectus	L	572	−12	42	−20	0.033
	Superior temporal gyrus	R	722	58	−38	12	0.034
	Superior orbital frontal gyrus	L	1443	−18	54	−14	0.034
	Angular gyrus	R	290	52	−48	28	0.036
	Supramarginal gyrus	R	272	60	−40	30	0.037
	Hippocampus	L	34	−22	−22	−10	0.044
White Matter	Superior longitudinal fasciculus	L	85,865	−44	−10	24	0.001
	Middle cerebellar preduncle	R	669	22	−62	−38	0.030
	Splenium of corpus callosum	R	485	14	−42	12	0.043

All clusters are FWE-corrected for multiple comparisons using TFCE.

inverted U-shaped pattern of development in GM with age, WM volume linearly increases throughout development until approximately young adulthood (Barnea-Goraly et al., 2005). Previous cross-sectional and longitudinal analyses revealed continuous age-related changes predominantly in the posterior parts of CC along with internal capsule (anterior corona radiata and frontal regions) (Giedd et al., 1999; Sowell et al., 1999). However, our results showing reduction in corpus callosum and superior longitudinal fasciculus have to be cautiously considered as the correlation between CogAGE and WM decrease in eigenvariates of those two clusters did not yield significant results. Taken together, our attempt to map cognitive development in CHR group onto neural substrates suggests that the interplay of strengthening and fine-tuning of relevant inter- and intra-hemispheric connections with elimination of GM occurs with delay in CHR patients relative to the healthy population. Speculatively, our results may point to a delay of oligodendrocyte-dependent axonal myelination (Peters and Sethares, 2004). Further research using advanced white matter imaging is needed to shed further light on this hypothesis.

The findings of this study should be considered in light of some limitations. First, our CogAGE model is cross-sectional and based on a limited age range of participants. Most participants were in their twenties at the time of their first scan and neurocognitive testing. Moreover, though we controlled for the age difference between the HC and CHR sample, the subsample of CHR-L that shows larger age range is limited in its number. Second, the number of CHR individuals from our sample that transited to psychosis was rather small ($N = 15$) and therefore comparisons between transition and non-transition groups need to be replicated in larger samples. While authors could not exclude the possibility that the study lacks sufficient power to detect differences in cognitive development between converters and non-converters the cognitive impairment is suggested to share a common ground in CHR individuals and psychosis patients. Our findings on significant negative relationship between CogAGE in CHR patients with more pronounced attenuated psychotic symptoms are pointing into this direction. Third, a patient group that has developed clinical symptoms to the level of psychosis would be helpful to determine the dynamic trajectory of cognitive development/maturation across the whole spectrum of psychosis.

Future studies will need to focus on using more sophisticated brain mapping methods and preferably longitudinal cohorts to determine dynamic trajectory of cognitive maturation in the whole spectrum of psychosis, early and late. However, our cross-sectional findings provide further evidence for aberrant brain structure-cognition associations in CHR state which supports the neurodevelopmental hypothesis of psychosis.

Conflict of interest

Acknowledgments

Appendix A. Supplementary data

Supplementary data to this article can be found online at https://doi.org/10.1016/j.nicl.2018.101624.

References

Albus, M., Hubmann, W., Mohr, F., et al., 2006. Neurocognitive functioning in patients with first-episode schizophrenia: results of a prospective 5-year follow-up study. Eur. Arch. Psychiatry Clin. Neurosci. 256 (7), 442–451. https://doi.org/10.1007/s00406-006-0667-1.

American Psychiatric Association, 2000. Diagnostic and statistical manual of mental disorders: DSM-IV-TR. American Psychiatric Association, Washington, DC.

Ashburner, J., 2007. A fast diffeomorphic image registration algorithm. NeuroImage 38 (1), 95–113. https://doi.org/10.1016/j.neuroimage.2007.07.007.

Ashburner, J., Friston, K.J., 2005. Unified segmentation. NeuroImage 26 (3), 839–851. https://doi.org/10.1016/j.neuroimage.2005.02.018.

Bachman, P., Niendam, T.A., Jalbrzikowski, M., et al., 2012. Processing speed and neurodevelopment in adolescent-onset psychosis: cognitive slowing predicts social function. J. Abnorm. Child Psychol. 40 (4), 645–654. https://doi.org/10.1007/s10802-011-9592-5.

Barnea-Goraly, N., Menon, V., Eckert, M., et al., 2005. White matter development during childhood and adolescence: a cross-sectional diffusion tensor imaging study. Cereb. Cortex 15 (12), 1848–1854. https://doi.org/10.1093/cercor/bhi062.

Cabral, C., Kambeitz-Ilankovic, L., Kambeitz, J., et al., 2016. Classifying schizophrenia using multimodal multivariate pattern recognition analysis: evaluating the impact of individual clinical profiles on the neurodiagnostic performance. Schizophr. Bull. 42 (Suppl. 1), S110–S117. https://doi.org/10.1093/schbul/sbw053.

Cropley, V.L., Klauser, P., Lenroot, R.K., et al., 2016. Accelerated gray and white matter

deterioration with age in schizophrenia. Am. J. Psychiatry 174 (3), 286–295. https://doi.org/10.1176/appi.ajp.2016.16050610.

Diedenhofen, B., Musch, J., 2015. cocor: a comprehensive solution for the statistical comparison of correlations. PLoS One 10 (4). https://doi.org/10.1371/journal.pone.0121945.

Erus, G., Battapady, H., Satterthwaite, T.D., et al., 2015. Imaging patterns of brain development and their relationship to cognition. Cereb. Cortex N Y N 25 (6), 1676–1684. https://doi.org/10.1093/cercor/bht425.

Gennatas, E.D., Avants, B.B., Wolf, D.H., et al., April 2017. Age-related effects and sex differences in gray matter density, volume, mass, and cortical thickness from childhood to young adulthood. J. Neurosci. https://doi.org/10.1523/JNEUROSCI.3550-16.2017. 3550-16.

Giedd, J.N., Blumenthal, J., Jeffries, N.O., et al., 1999. Brain development during childhood and adolescence: a longitudinal MRI study. Nat. Neurosci. 2 (10), 861. https://doi.org/10.1038/13158.

Gogtay, N., 2008. Cortical brain development in schizophrenia: insights from neuroimaging studies in childhood-onset schizophrenia. Schizophr. Bull. 34 (1), 30–36. https://doi.org/10.1093/schbul/sbm103.

Green, M.F., Horan, W.P., Lee, J., 2015. Social cognition in schizophrenia. Nat. Rev. Neurosci. 16 (10), 620–631. https://doi.org/10.1038/nrn4005.

Gur, R.C., Calkins, M.E., Satterthwaite, T.D., et al., 2014. Neurocognitive growth charting in psychosis spectrum youths. JAMA Psychiatry 71 (4), 366–374. https://doi.org/10.1001/jamapsychiatry.2013.4190.

Holm, S., 1979. A simple sequentially rejective multiple test procedure. Scand. J. Stat. 6 (2), 65–70.

Kay, S.R., Flszbein, A., Opfer, L.A., 1987. The positive and negative syndrome scale (PANSS) for schizophrenia. Schizophr. Bull. 13 (2), 261–276.

Keefe, R.S.E., Perkins, D.O., Gu, H., Zipursky, R.B., Christensen, B.K., Lieberman, J.A., 2006. A longitudinal study of neurocognitive function in individuals at-risk for psychosis. Schizophr. Res. 88 (1–3), 26–35. https://doi.org/10.1016/j.schres.2006.06.041.

Khandaker, G.M., Barnett, J.H., White, I.R., Jones, P.B., 2011. A quantitative meta-analysis of population-based studies of premorbid intelligence and schizophrenia. Schizophr. Res. 132 (2–3), 220–227. https://doi.org/10.1016/j.schres.2011.06.017.

Klosterkötter, J., Hellmich, M., Steinmeyer, E.M., Schultze-Lutter, F., 2001. Diagnosing schizophrenia in the initial prodromal phase. Arch. Gen. Psychiatry 58 (2), 158–164.

Koutsouleris, N., Patschurek-Kliche, K., Scheuerecker, J., et al., 2010. Neuroanatomical correlates of executive dysfunction in the at-risk mental state for psychosis. Schizophr. Res. 123 (2–3), 160–174. https://doi.org/10.1016/j.schres.2010.08.026.

Koutsouleris, N., Borgwardt, S., Meisenzahl, E.M., Bottlender, R., Möller, H.-J., Riecher-Rössler, A., 2012a. Disease prediction in the at-risk mental state for psychosis using neuroanatomical biomarkers: results from the FePsy study. Schizophr. Bull. 38 (6), 1234–1246. https://doi.org/10.1093/schbul/sbr145.

Koutsouleris, N., Davatzikos, C., Bottlender, R., et al., 2012b. Early recognition and disease prediction in the at-risk mental states for psychosis using neurocognitive pattern classification. Schizophr. Bull. 38 (6), 1200–1215. https://doi.org/10.1093/schbul/sbr037.

Koutsouleris, N., Davatzikos, C., Borgwardt, S., et al., 2014. Accelerated brain aging in schizophrenia and beyond: a neuroanatomical marker of psychiatric disorders. Schizophr. Bull. 40 (5), 1140–1153. https://doi.org/10.1093/schbul/sbt142.

Koutsouleris, N., Riecher-Rössler, A., Meisenzahl, E.M., et al., 2015. Detecting the psychosis prodrome across high-risk populations using neuroanatomical biomarkers. Schizophr. Bull. 41 (2), 471–482. https://doi.org/10.1093/schbul/sbu078.

Lieberman, J.A., 1999. Is schizophrenia a neurodegenerative disorder? A clinical and neurobiological perspective. Biol. Psychiatry 46 (6), 729–739.

Lin, A., Wood, S.J., Nelson, B., et al., 2011. Neurocognitive predictors of functional outcome two to 13 years after identification as ultra-high risk for psychosis. Schizophr. Res. 132 (1), 1–7. https://doi.org/10.1016/j.schres.2011.06.014.

Luna, B., Garver, K.E., Urban, T.A., Lazar, N.A., Sweeney, J.A., 2004. Maturation of cognitive processes from late childhood to adulthood. Child Dev. 75 (5), 1357–1372. https://doi.org/10.1111/j.1467-8624.2004.00745.x.

Manjón, J.V., Tohka, J., Robles, M., 2010. Improved estimates of partial volume coefficients from noisy brain MRI using spatial context. NeuroImage 53 (2), 480–490. https://doi.org/10.1016/j.neuroimage.2010.06.046.

Marder, S.R., Fenton, W., 2004. Measurement and treatment research to improve cognition in schizophrenia: NIMH MATRICS initiative to support the development of agents for improving cognition in schizophrenia. Schizophr. Res. 72 (1), 5–9. https://doi.org/10.1016/j.schres.2004.09.010.

Meisenzahl, E.M., Koutsouleris, N., Gaser, C., et al., 2008. Structural brain alterations in

subjects at high-risk of psychosis: a voxel-based morphometric study. Schizophr. Res. 102 (1–3), 150–162. https://doi.org/10.1016/j.schres.2008.02.023.

Montgomery, S.A., Asberg, M., 1979. A new depression scale designed to be sensitive to change. Br. J. Psychiatry 134 (4), 382–389. https://doi.org/10.1192/bjp.134.4.382.

Moore, T.M., Reise, S.P., Gur, R.E., Hakonarson, H., Gur, R.C., 2015. Psychometric properties of the Penn computerized neurocognitive battery. Neuropsychology 29 (2), 235. https://doi.org/10.1037/neu0000093.

Pantelis, C., Yücel, M., Wood, S.J., et al., 2005. Structural brain imaging evidence for multiple pathological processes at different stages of brain development in schizophrenia. Schizophr. Bull. 31 (3), 672–696. https://doi.org/10.1093/schbul/sbi034.

Peters, A., Sethares, C., 2004. Oligodendrocytes, their progenitors and other neuroglial cells in the aging primate cerebral cortex. Cereb. Cortex N Y N 14 (9), 995–1007. https://doi.org/10.1093/cercor/bhh060.

Pukrop, R., Schultze-Lutter, F., Ruhrmann, S., et al., 2006. Neurocognitive functioning in subjects at risk for a first episode of psychosis compared with first- and multiple-episode schizophrenia. J. Clin. Exp. Neuropsychol. 28 (8), 1388–1407. https://doi.org/10.1080/13803390500434425.

Rajapakse, J.C., Giedd, J.N., Rapoport, J.L., 1997. Statistical approach to segmentation of single-channel cerebral MR images. IEEE Trans. Med. Imaging 16 (2), 176–186. https://doi.org/10.1109/42.563663.

Rapoport, J.L., Giedd, J.N., Gogtay, N., 2012. Neurodevelopmental model of schizophrenia: update 2012. Mol. Psychiatry 17 (12), 1228–1238. https://doi.org/10.1038/mp.2012.23.

Reichenberg, A., Weiser, M., Rabinowitz, J., et al., 2002. A population-based cohort study of premorbid intellectual, language, and behavioral functioning in patients with schizophrenia, schizoaffective disorder, and nonpsychotic bipolar disorder. Am. J. Psychiatry 159 (12), 2027–2035.

Saeys, Y., Inza, I., Larrañaga, P., 2007. A review of feature selection techniques in bioinformatics. Bioinforma Oxf. Engl. 23 (19), 2507–2517. https://doi.org/10.1093/bioinformatics/btm344.

Schnack, H.G., van Haren, N.E.M., Nieuwenhuis, M., Hulshoff Pol, H.E., Cahn, W., Kahn, R.S., Jun 1, 2016. Accelerated Brain Aging in Schizophrenia: a Longitudinal Pattern Recognition Study. Am. J. Psychiatry 173 (6), 607–616. https://doi.org/10.1176/appi.ajp.2015.15070922. Epub 2016 Feb 26.

Smith, S.M., Nichols, T.E., 2009. Threshold-free cluster enhancement: addressing problems of smoothing, threshold dependence and localisation in cluster inference. NeuroImage 44 (1), 83–98. https://doi.org/10.1016/j.neuroimage.2008.03.061.

Sowell, E.R., Thompson, P.M., Holmes, C.J., Batth, R., Jernigan, T.L., Toga, A.W., 1999. Localizing age-related changes in brain structure between childhood and adolescence using statistical parametric mapping. NeuroImage 9 (6), 587–597. https://doi.org/10.1006/nimg.1999.0436. Pt 1.

Su, L., Wang, L., Hu, D., 2012. Predicting the age of healthy adults from structural mri by sparse representation. In: Intelligent Science and Intelligent Data Engineering. Lecture Notes in Computer Science. Springer, Berlin, Heidelberg, pp. 271–279. https://doi.org/10.1007/978-3-642-36669-7_34.

Sussman, D., Leung, R.C., Chakravarty, M.M., Lerch, J.P., Taylor, M.J., 2016. The developing human brain: age-related changes in cortical, subcortical, and cerebellar anatomy. Brain Behav. 6 (4). https://doi.org/10.1002/brb3.457.

Tiemeier, H., Lenroot, R.K., Greenstein, D.K., Tran, L., Pierson, R., Giedd, J.N., 2010. Cerebellum development during childhood and adolescence: a longitudinal morphometric MRI study. NeuroImage 49 (1), 63–70. https://doi.org/10.1016/j.neuroimage.2009.08.016.

Tohka, J., Zijdenbos, A., Evans, A., 2004. Fast and robust parameter estimation for statistical partial volume models in brain MRI. NeuroImage 23 (1), 84–97. https://doi.org/10.1016/j.neuroimage.2004.05.007.

Woods, B.T., 1998. Is schizophrenia a progressive neurodevelopmental disorder? Toward a unitary pathogenetic mechanism. Am. J. Psychiatry 155 (12), 1661–1670. https://doi.org/10.1176/ajp.155.12.1661.

Yung, A.R., Phillips, L.J., McGorry, P.D., et al., 1998. Prediction of psychosis. A step towards indicated prevention of schizophrenia. Br. J. Psychiatry Suppl. 172 (33), 14–20.

Yung, A.R., Phillips, L.J., Yuen, H.P., et al., 2003. Psychosis prediction: 12-month follow up of a high-risk ("prodromal") group. Schizophr. Res. 60 (1), 21–32.

Yung, A.R., Phillips, L.J., Yuen, H.P., McGorry, P.D., 2004. Risk factors for psychosis in an ultra high-risk group: psychopathology and clinical features. Schizophr. Res. 67 (2–3), 131–142. https://doi.org/10.1016/S0920-9964(03)00192-0.

Ziermans, T., De, Wit S., Schothorst, P., et al., 2014. Neurocognitive and clinical predictors of long-term outcome in adolescents at ultra-high risk for psychosis: a 6-year follow-up. PLoS One 9 (4), e93994. https://doi.org/10.1371/journal.pone.0093994.